



# Effects of the Invasion of *Caulerpa cylindracea* in a *Cymodocea nodosa* Meadow in the Northern Adriatic Sea

Mirjana Najdek<sup>1\*</sup>, Marino Korlević<sup>1</sup>, Paolo Paliaga<sup>2</sup>, Marsej Markovski<sup>1</sup>, Ingrid Ivančić<sup>1</sup>, Ljiljana Iveša<sup>1</sup>, Igor Felja<sup>3</sup> and Gerhard J. Herndl<sup>4,5</sup>

<sup>1</sup> Center for Marine Research, Ruder Bošković Institute, Zagreb, Croatia, <sup>2</sup> Department of Natural and Health Sciences, University of Pula, Pula, Croatia, <sup>3</sup> Department of Geology, Faculty of Science, University of Zagreb, Zagreb, Croatia, <sup>4</sup> Department of Functional and Evolutionary Ecology, Faculty of Life Sciences, University of Vienna, Vienna, Austria, <sup>5</sup> Department of Marine Microbiology and Biogeochemistry, NIOZ Royal Netherlands Institute for Sea Research, Utrecht University, Den Burg, Netherlands

## OPEN ACCESS

### Edited by:

Johan Schijf,  
University of Maryland Center  
for Environmental Science (UMCES),  
United States

### Reviewed by:

Zhijian Jiang,  
Chinese Academy of Sciences, China  
Gloria Peralta,  
University of Cádiz, Spain  
Jaime Bernardeau,  
Instituto Español de Oceanografía,  
Spain

### \*Correspondence:

Mirjana Najdek  
najdek@cim.irb.hr

### Specialty section:

This article was submitted to  
Marine Biogeochemistry,  
a section of the journal  
Frontiers in Marine Science

**Received:** 02 September 2020

**Accepted:** 26 November 2020

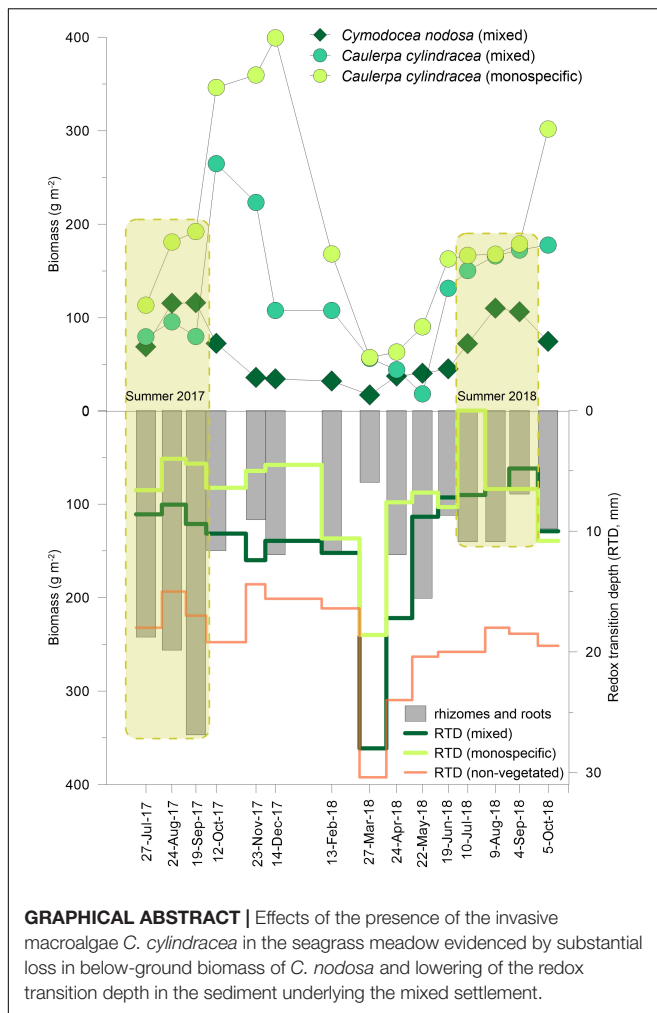
**Published:** 23 December 2020

### Citation:

Najdek M, Korlević M, Paliaga P,  
Markovski M, Ivančić I, Iveša L, Felja I  
and Herndl GJ (2020) Effects of the  
Invasion of *Caulerpa cylindracea* in a  
*Cymodocea nodosa* Meadow  
in the Northern Adriatic Sea.  
Front. Mar. Sci. 7:602055.  
doi: 10.3389/fmars.2020.602055

The effect of the presence of invasive macroalgae *Caulerpa cylindracea* Sonder in the seagrass meadow *Cymodocea nodosa* (Ucria) Ascherson was studied by comparing the dynamics of biological and physicochemical parameters in the tissues of these two macrophytes and in the sediments underlying an invaded meadow (mixed settlement) and a *C. cylindracea* monospecific settlement. The study was conducted for 15 months, encompassing two summers during 2017 and 2018 (July to September) when maximum *C. nodosa* growth occurs. During 2017 *C. cylindracea* biomasses in the mixed settlement ( $79.5 \pm 28.2$  to  $264.6 \pm 65.1$  g m<sup>-2</sup>) were lower than in its monospecific stands ( $113.4 \pm 48.0$  to  $399.3 \pm 56.3$  g m<sup>-2</sup>). In the same period, less reducing conditions in the sediment underlying the mixed settlement were indicated by deeper redox transition depths (RTD: 8–12 mm) than those observed below the *C. cylindracea* monospecific settlement (RTD: 4–7 mm). In June 2018, *C. cylindracea* proliferated in both settlements reaching very similar biomasses that were maintained until September 2018 (mixed:  $131.5 \pm 23.0$  to  $172.5 \pm 16.3$  g m<sup>-2</sup>; monospecific:  $162.8 \pm 32.5$  to  $178.8 \pm 30.0$  g m<sup>-2</sup>). In parallel, a considerable lowering of RTD (5–7 mm) under the mixed settlement indicated the progression of stronger reducing conditions similar to those observed under the monospecific settlement (RTD: 0–7 mm). This alteration was followed by a decrease in *C. nodosa* below-ground biomass ( $89.3 \pm 16.0$  to  $140.3 \pm 24.3$  g m<sup>-2</sup>), that became considerably lower than in the same period of 2017 ( $242.3 \pm 44.3$  to  $346.9 \pm 32.1$  g m<sup>-2</sup>). At the same time, the above-ground biomass of *C. nodosa* ( $72.3 \pm 14.8$  to  $110.3 \pm 13.4$  g m<sup>-2</sup>) showed no difference to the summer of 2017 ( $69.0 \pm 15.4$  to  $116.0 \pm 37.4$  g m<sup>-2</sup>). The resulting increase of the above- to below-ground biomass ratio indicated the disruption of the meadow stability. More intense spawning of *C. cylindracea* in the mixed settlement during the summer 2018 hindered its expected proliferation in October 2018, while the below-ground biomass of *C. nodosa* increased concomitantly with the deepening of the RTD suggesting a possible recovery of the meadow stability.

**Keywords:** *Caulerpa cylindracea*, *Cymodocea nodosa*, invaded seagrass meadow, sediment biogeochemistry, northern Adriatic Sea, seagrass meadow stability



## INTRODUCTION

Seagrasses are one of the most important habitat-forming species in Mediterranean coastal areas and play a key role in the preservation of marine biodiversity and carbon sequestration (Duarte et al., 2013; Samper-Villarreal et al., 2016). They can be threatened by nutrient loading, warming, sediment runoff, physical disturbance, intense grazing, algal blooms, and invasion by non-indigenous species (Orth et al., 2006; Rasheed and Unsworth, 2011; Marín-Guirao et al., 2015, 2016; Nguyen et al., 2020). Generally, the introduction of the tropical invasive macroalgae of the genus *Caulerpa* in the Mediterranean Sea was recognized as a significant environmental concern due to its modification of benthic communities and reduction of biodiversity on large spatial scales (Piazzi et al., 2001; Boudouresque et al., 2009; Piazzi and Balata, 2009; Bulleri et al., 2010; Tamburello et al., 2015).

Invasive *Caulerpa* species can strongly compete with native species in temperate areas, leading to their decline and constituting monospecific beds (Piazzi et al., 2001). In seagrass habitats, this alga overgrows their rhizomes; interacting in both the below- and above-ground tissues, affecting nutrient

acquisition and light availability (Ceccherelli et al., 2000). In contrast, seagrass provides a sub-canopy microhabitat to *Caulerpa* sp. that differs from the non-vegetated sediment being characterized by canopy shading (Ceccherelli and Cinelli, 1999), slowing down water motion (Gambi et al., 1990) and releasing secondary metabolites that can interfere with understory species and grazers. In temperate areas, the extensive spreading of *Caulerpa* was ascribed to the successful adaptation to seasonal changes in environmental conditions (Khotimchenko, 1995; Iveša et al., 2004; Blažina et al., 2009) in addition to both modes of propagation, by vegetative and sexual reproduction (Panayotidis and Žuljević, 2001). Numerous short-term studies relate the presence of *Caulerpa* to deterioration processes of seagrass meadows, by competitive displacement or by altering the sediment quality which becomes more suitable for the invasive macroalgae growth (De Villèle and Verlaque, 1995; Ceccherelli and Cinelli, 1997; Holmer et al., 2009).

The sediments underlying seagrasses are generally less hypoxic, present lower levels of nitrogen fixation and lower sulfide concentrations than those settled by *Caulerpa* sp. (Chisholm and Moulin, 2003; Garcias-Bonet et al., 2008; Holmer et al., 2009; McKinnon et al., 2009; Gallucci et al., 2012; Gribben et al., 2018). The presence of *Caulerpa* modifies benthic microbial community composition (Rizzo et al., 2017), as well as patterns of bacterially mediated organic matter diagenesis by stimulating  $N_2$  fixation due to the release of secondary metabolites through plant rhizoids (Chisholm and Moulin, 2003), and modifying other microbial processes in the sediments. Sulfate-reducing bacteria elevate the sulfate reduction rates and  $H_2S$  production in such sediments. Hydrogen sulfide is highly toxic to plants, and its possible intrusion into their tissues may reduce the growth and survival of the seagrass (Garcias-Bonet et al., 2008).

*Caulerpa cylindracea* Sonder was first identified in the year 2000 in the central Adriatic (Žuljević et al., 2003) and successively spread north reaching the coldest area of its expansion in the Mediterranean (Iveša and Devescovi, 2006). This invasive macroalgae colonized all kinds of substrates, from rocky bottoms to seagrass meadows (Iveša and Devescovi, 2006; Iveša et al., 2015). Given the wide distribution of *C. cylindracea* along the ecological status of seagrass meadows in this area, a study was conducted to investigate the growth cycle of *C. cylindracea* in the seagrass meadow *Cymodocea nodosa* (Ucria) Ascherson and the possible effect of their interactions on the sediment's physico-chemical properties. We hypothesized that the presence of *C. cylindracea* can disturb the stability of the *C. nodosa* meadow by modifying the sediment conditions that concurrently favor the growth of *C. cylindracea* and limit it for *C. nodosa*. An effect of the presence of *C. cylindracea* in the *C. nodosa* meadow was evaluated by comparing the physiological and growth state of the macrophytes, environmental conditions in the water column and sediment between the summer of 2017 and the summer of 2018, the periods of *C. nodosa* maximum growth. This study aims to offer further insights to the complex interactions between invasive and native macrophytes and their relative importance in the maintenance of the seagrass habitat stability.

## MATERIALS AND METHODS

### Study Site and Samplings

Funtana Bay is located along the western coast of Istria (Croatia) in the northern Adriatic, 30 km northwest of Rovinj (45°10'42"N; 13°35'51"E, **Figure 1**). The coast of Funtana Bay is rocky, moderately indented, and partially exposed to waves coming from the west and northwest. The sea floor is partly overgrown with *C. cylindracea*, which can be found alone or mixed with the seagrass *C. nodosa*. A monthly field survey was carried out from July 2017 to October 2018. Samplings were performed at three proximate sites; in the *C. nodosa* meadow invaded by the green macroalgae *C. cylindracea* (mixed settlement, sampling depth: 2–2.5 m), in the *C. cylindracea* settlement (monospecific settlement, sampling depth: 1–1.5 m) and in a non-vegetated area (sampling depth: 1–1.5 m).

Seawater for nutrients, chlorophyll *a* (Chl *a*), particulate matter (PM) concentration, and prokaryotic abundance (PA) analysis was collected with plastic bottles (10 L). *C. nodosa* (with rhizomes and roots), *C. cylindracea* thalli, and macroalgae were collected by snorkeling using three square frames (20 × 20 cm) scattered randomly in the areas of highest vegetation presence. Sediment samples were collected within the vegetated (mixed and monospecific settlement) and in the non-vegetated sediment by divers using plastic corers (length, 15 cm; area 15.9 cm<sup>2</sup>). The cores for granulometric composition, total lipids, and PA were cut into 1 cm sections and lyophilized with the exception of sections used for determining the abundance of prokaryotes which were weighed (2 g) and fixed with formaldehyde (final conc. 4% v/v).

### Environmental Parameters

Temperature (T) was continuously measured at 30 min. intervals by HOBO pendant Temp/Light Data Loggers (Onset, United States) placed in the mixed and monospecific settlement. Salinity (S) was measured on each sampling by a pIONeer 65 probe (Radiometer analytical, Copenhagen). Nutrients (NO<sub>3</sub>, NO<sub>2</sub>, NH<sub>4</sub>, PO<sub>4</sub>, and SiO<sub>4</sub>) were analyzed according to Strickland and Parsons (1972). Chl *a* was determined using a fluorometer after seawater filtration through a Whatman GF/F filter (Holm-Hansen et al., 1965). Particulate matter (PM) was determined by weighing after filtering 5 L of seawater on pre-weighed, combusted Whatman GF/F filters, and dried at 60°C.

### Prokaryotic Abundance Determination

Prokaryotic abundance in seawater was determined after fixing 2 mL of samples with formaldehyde (final conc. 4% v/v) and staining with 4,6-diamidino-2-phenylindol (DAPI, 1 μg mL<sup>-1</sup> final conc.) for 10 min (Porter and Feig, 1980). Prokaryotes in sediments were detached by adding Tween 80 (50 μL) and ultrasonicated for 15 min (Epstein and Rossel, 1995). After the sonication, DAPI (final conc. 5 μg/mL) was added to 1 mL of the supernatant. Samples stained with DAPI were then filtered through black polycarbonate filters (Whatman, Nuclepore, 0.22 μm) and prokaryotes were counted under an epifluorescence microscope (Zeiss Axio Imager Z1).

### Biometry of Macrophytes

The macrophytes from each square were thoroughly washed with seawater to eliminate the associated sediment, and separated into three groups of macrophytes: *C. cylindracea* thalli, *C. nodosa* (leaves and rhizomes with roots), and macroalgae thalli. For *C. nodosa*, shoots were counted and the length of the longest leaf of each shoot was measured. Macroalgae from each sample were placed on the surface that has an area equal to the sample *in situ* (20 × 20 cm) and identified to species level. The cover of each thallus, representing the surface covered in orthogonal projection, was determined according to Cormaci et al. (2004). Species of macroalgae were affiliated to the following morpho-functional groups: corticated, articulated calcareous, filamentous, foliose, leathery, and crustose (Littler and Littler, 1984). Individual samples were rinsed again, weighed, dried at 60°C for 48 h, re-weighed, and the dry mass expressed in g m<sup>-2</sup>.

### Sediment Granulometric Composition

Each sample was wet sieved through standard ASTM sieves (4-, 2-, 1-, 0.5-, 0.25-, 0.125-, 0.063-mm mesh size). The fraction passing through the 0.063-mm sieve was analyzed according to standard sedigraph procedures (MICROMERITICS, 2002). The retained particles were dried and weighed. Merging the data acquired by both techniques a continuous grain size range was obtained, analyzed with the statistic package Gradistat v 6.0, and classified according to Folk (1954). Sediment permeability was calculated following the empirical relation by Gangi (1985) based on the median grain size ( $d_g$ ):  $k = Dar \cdot 735 \cdot 10^6 \cdot d_g^2$ , where  $k$  is the permeability in m<sup>2</sup> and  $Dar$  is the conversion factor for unit Darcy into m<sup>2</sup> ( $=9.869 \cdot 10^{-13}$ ).

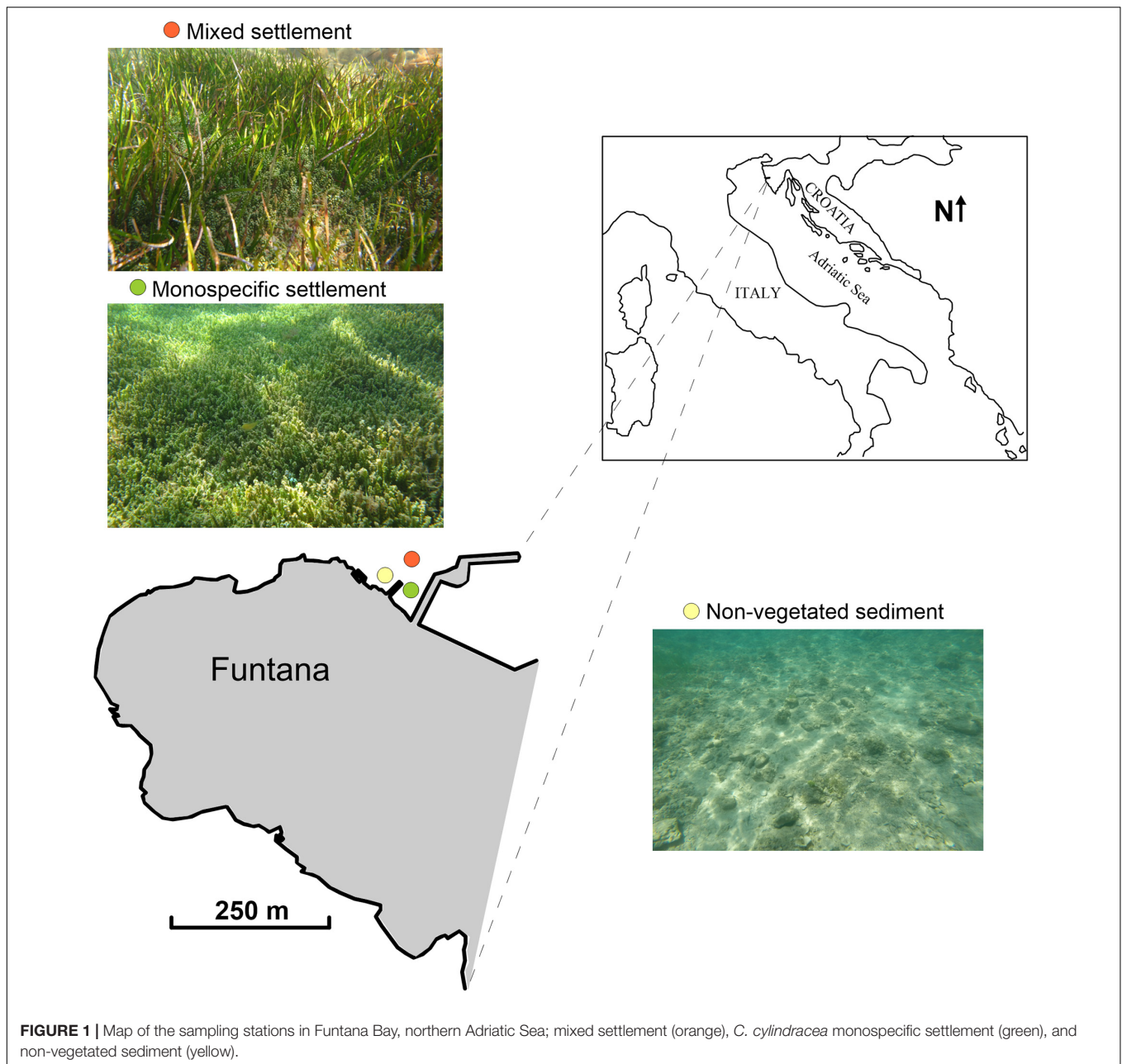
### Oxygen (O<sub>2</sub>), Hydrogen Sulfide (H<sub>2</sub>S), and Redox Potential (Eh)

The vertical distribution of O<sub>2</sub>, H<sub>2</sub>S, and Eh was measured in sediment cores using a motorized micromanipulator (MMS9083) equipped with OX-100 and H<sub>2</sub>S-200 microsensors probes, and a redox microelectrode RD-200 coupled with the reference electrode REF-RM (Unisense A/S, Denmark). All microsensors probes were calibrated according to the manufacturer's instructions. The OX-100 probe was calibrated with a two-point oxic–anoxic calibration, H<sub>2</sub>S-200 with eight-point calibration in fresh Na<sub>2</sub>S solutions [1–300 μM in a de-oxygenated calibration buffer (NaAc/HAc, pH < 4)], RD-200 coupled with REF-RM by a two-point calibration using synchronized immersion of electrodes in quinhydrone redox solutions in pH 4 and pH 7 buffers. During measurements, *in situ* temperature was maintained by keeping the sediment cores in a glass container filled with seawater from the sampling location. From July to October 2017, H<sub>2</sub>S in pore waters centrifuged from 5 mm sediment cores section was measured according to Cline (1969).

### Total Lipids, Fatty Acid Composition, and Sulfur

The detailed procedure for determination of total lipids (TL), fatty acid composition [fatty acid methyl esters (FAME)],





and elemental sulfur ( $S^0$ ) was reported previously (Najdek et al., 2020). Briefly, lyophilized samples were weighed and consecutively ultrasonically extracted into a solvent mixture of dichloromethane/methanol (DCM: MeOH, 2:1) and separated into layers. Lipid containing layers were evaporated to dryness and weighed. The fatty acid composition was determined from lipid extracts, after saponification, acidification, methylation, and extraction in DCM.

Fatty acid methyl esters were analyzed by an Agilent gas-liquid chromatography (GLC) 6890 N GC System with a 5973 Network Mass Selective Detector, capillary column (30 m × 0.3 mm × 0.25 μm; cross-linked 5% phenylmethylsiloxane) and ultra-high purity helium as the

carrier gas. The GLC settings were: programmed column temperature increase from 145 to 215°C by 4°C/min, then by 1°C/min to 225°C, and by 4°C/min to 270°C at constant column pressure of 2.17 kPa. The concentration of elemental sulfur ( $S^0$ ) in FAME chromatograms was estimated using the calibration curve determined under the same GLC settings as FAME.

## Data Analyses

Analysis of variance (ANOVA) was performed by GMAV5 for Windows. The effects of factors settlements (mixed and monospecific), summer (2017 and 2018), and sampling months (July, August, and September) on the biomasses of *C. cylindracea* and macroalgae were tested by three-way ANOVA. The effects

of factors summer (2017 and 2018) and sampling months (July, August, and September) on the above-ground biomass, below-ground biomass, shoot density, and the longest leaf length of *C. nodosa* were tested by two-way ANOVA. In addition, the effects of factors sampling site (mixed, monospecific, and non-vegetated) and summer (2017 and 2018) on total lipid and prokaryotes concentration in the sediment were tested by two-way ANOVA. Homogeneity of variances was tested by Cochran's test. Significant ANOVA results ( $p < 0.05$ ) were followed with *post hoc* Student–Newman–Keuls (SNK) test. Correlations were tested using Pearson's correlation coefficient ( $r$ ) with a level of statistical significance,  $p < 0.05$ . Only sediment samples originating from the upper part of cores (0–4 cm), where most rhizomes and roots reside, were used for analyses. A multivariate principal component analysis (PCA, Primer 6) was used to recognize the most important variables which explained the differences between vegetated sediments. Correlation matrices were based on  $H_2S$ ,  $S^0$ , Eh,  $O_2$ , TL, and PAs as variables, which were normalized due to their different scales. Only the principal components with eigenvalues  $> 1$  were considered.

## RESULTS

### Environmental Variables

During the summer of 2017, daily means of sea-bottom temperature ranged between 26 and 28°C. During autumn and winter, seawater temperatures decreased. The coldest period was recorded at the end of February 2018, with minima of 8.49 and 8.26°C in the mixed and monospecific settlement, respectively, but it lasted only a few days. After a steep increase from April to June 2018, in August 2018, the temperature reached with large fluctuations a maximum of 29.34°C in the mixed and 28.84°C in the monospecific settlement (Figure 2A). The fluctuations in daily temperatures relative to the monthly averages over the sampling period July/August 2017 were considerably lower (up to 1°C) and more uniform than those obtained for July/August 2018 (up to 3°C) (Figure 2B). The temperature conditions in the mixed settlement were more variable than in the monospecific settlement. Half-hourly values were up to 1.34°C higher during the day and up to 1.12°C lower during the night in the mixed than in the monospecific settlement (Figure 2C).

Concentrations of inorganic nutrients (DIN: 1.07–3.40  $\mu M$ ;  $PO_4$ : 0–0.08  $\mu M$ ;  $SiO_4$ : 1.24–3.21  $\mu M$ ; and Chl *a* (0.26–0.85  $\mu g L^{-1}$ ) in Funtana bay were generally low. The abundance of prokaryotes in the ambient water ( $2.8$ – $8.9 \times 10^5$  cell  $mL^{-1}$ ) correlated with seawater temperature ( $r = 0.618$ ;  $p < 0.05$ ) and PM ( $4.94$ – $15.47$  mg  $L^{-1}$ ) with Chl *a* ( $r = 0.49$ ,  $p < 0.05$ ). The variations in salinity (S: 35.5–38.5) were irregular, with the lowest values between August and October 2018 (Supplementary Table S1).

### Biometry

*Cymodocea nodosa* (Figure 3A) showed a regular seasonal fluctuation in biomass, leaf length, and shoot density which peaked in summer 2017 and 2018 (up to  $116.0 \pm 27.5$  g  $m^{-2}$ ,  $130.6 \pm 20.6$  mm, and  $2043 \pm 100$  shoots  $m^{-2}$ , respectively) and decreased in winter/early spring (down to  $17.5 \pm 4.0$  g  $m^{-2}$ ,

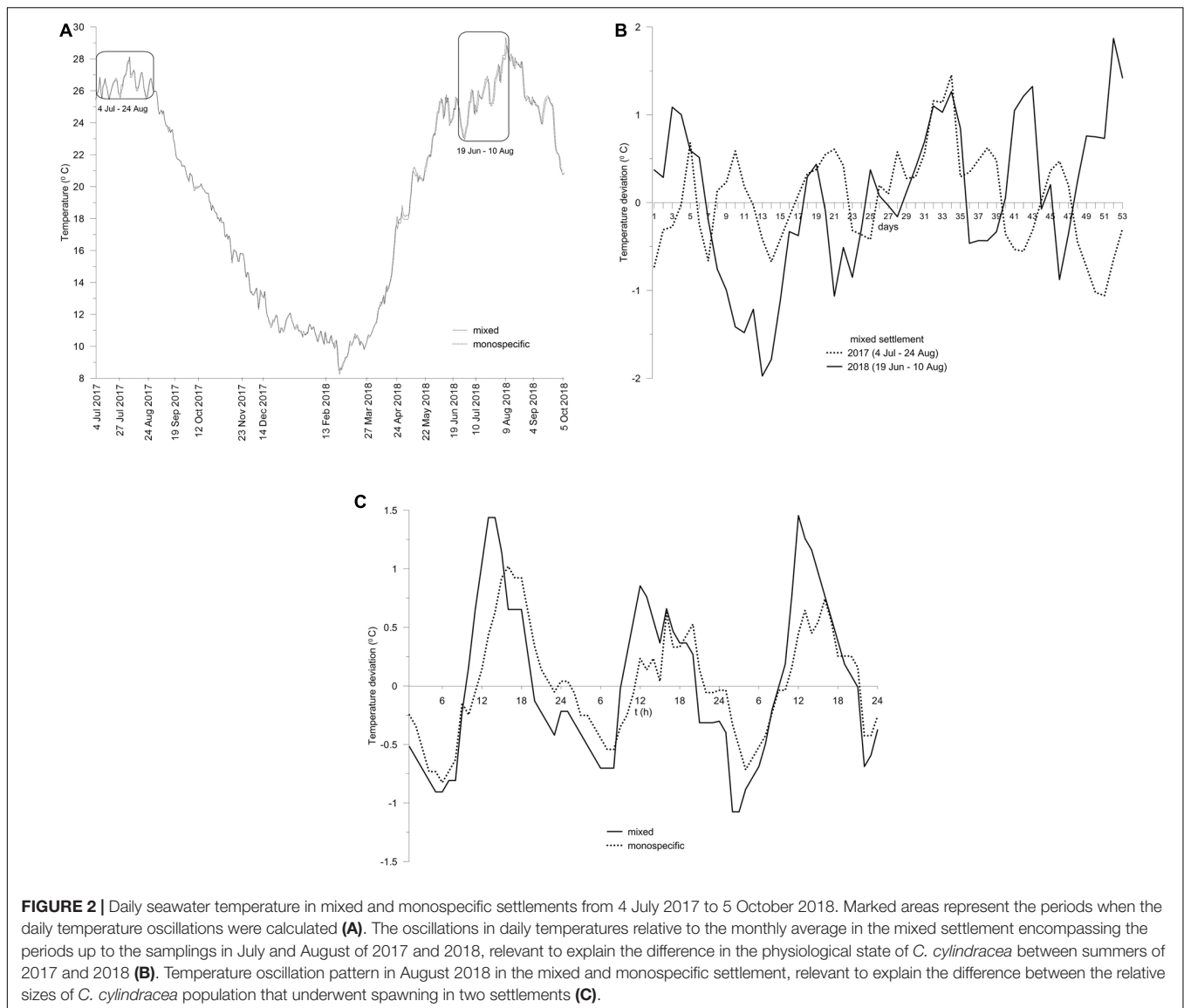
$52.6 \pm 23.8$  mm, and  $42 \pm 62$  shoots  $m^{-2}$ , respectively). In the summer of 2017, the *C. nodosa* above-ground biomass, the leaves length, and shoot density were not significantly different from those measured during summer 2018 (Supplementary Tables S2, S3). The biomasses of rhizomes and roots reached their maximum during summer 2017 (up to  $346.9 \pm 32.1$  g  $m^{-2}$ ). After the winter minimum (down to  $76.7 \pm 45.0$  g  $m^{-2}$ ), the below-ground biomass increased until May 2018 ( $254.8 \pm 33.7$  g  $m^{-2}$ ), then decreased until September 2018 ( $89.3 \pm 16.0$  g  $m^{-2}$ ), and began to increase again in October 2018 ( $122.3 \pm 24.12$  g  $m^{-2}$ ). During summer 2018, the below-ground biomass was significantly lower than in the summer of 2017 (Supplementary Table S2).

In the mixed settlement (Figure 3B), *C. cylindracea* biomass peaked in October 2017 ( $264.7 \pm 65.1$  g  $m^{-2}$ ). After a significant decline in December 2017 ( $107.7 \pm 19.5$  g  $m^{-2}$ ), biomass reached a minimum in May 2018 ( $18.5 \pm 4.5$  g  $m^{-2}$ ). Following the increase in June 2018 ( $131.5 \pm 23.5$  g  $m^{-2}$ ), the biomass moderately increased until October 2018 ( $177.7 \pm 13.2$  g  $m^{-2}$ ). In the monospecific settlement, *C. cylindracea* biomass rapidly increased in October 2017 ( $346.3 \pm 69.7$  g  $m^{-2}$ ), gradually reaching its maximum in December 2017 ( $399.2 \pm 56.3$  g  $m^{-2}$ ). After the minimum in March 2018 ( $57.5 \pm 32.3$  g  $m^{-2}$ ), the biomass increased in June 2018 ( $162.7 \pm 32.5$  g  $m^{-2}$ ), and remained fairly stable until a considerable increase in October 2018 ( $301.7 \pm 24.5$  g  $m^{-2}$ ). During the summer of 2017, *C. cylindracea* biomass in the mixed settlement was significantly lower than in the monospecific settlement, while in 2018, no significant difference in biomass between the two settlements was observed (Supplementary Table S4).

In the mixed and monospecific settlements, similar macroalgae taxa were present throughout the study period. The corticated *Rytiphlaea tinctoria* (Rhodophyta), foliose *Udotea petiolata* (Chlorophyta), and articulated calcareous *Halimeda tuna* (Chlorophyta) algae were almost always present in the both settlements (Supplementary Table S5). Filamentous macroalgae (*Cladophora* sp., *Polysiphonia* sp.) generally contributed more to the macroalgae cover of the mixed settlement, while their presence with a higher coverage in both settlements was observed during the summer 2018 (Supplementary Figure S1). The macroalgae biomass in the monospecific settlement was significantly lower than in the mixed settlement whereas no differences between two summers were observed (Supplementary Table S4). In both settlements, the highest macroalgae biomass was recorded in October 2017 (mixed:  $173.5 \pm 14.2$  g  $m^{-2}$  and monospecific:  $130.7 \pm 9.8$  g  $m^{-2}$ ). In the mixed settlement, a macroalgae biomass increase ( $169.3 \pm 15.0$  g  $m^{-2}$ ) was also observed in April 2018 with a presence and higher coverage of filamentous macroalgae, particularly *Cladophora prolifera*, in contrast to the monospecific settlement (Figure 3C and Supplementary Figure S1).

### Total Lipid (TL) Concentrations and Fatty Acid Composition

TL in the *C. nodosa* leaves ( $11.5 \pm 2.6$  to  $29.6 \pm 3.1$  mg  $g^{-1}$  dry weight, DW) showed two maxima, in March and August 2018, while the minimum was measured in November



2017 (Figure 4A). The major fatty acid components were palmitic (C16:0) among the saturated (SAT), oleic (C18:1n-9) in monounsaturated fatty acids (MUFA) and  $\alpha$ -linolenic (C18:3 n-3, ALA) in polyunsaturated fatty acids (PUFA). ALA generated a pattern of PUFA and the unsaturation degree (UND) dynamics. PUFA and UND were high (61.5–65.9% and 5.29–6.43, respectively) during the summer of 2017 and decreased toward November 2017 (55.6%, 4.21). From December 2017 onward, PUFA and UND increased and reached a maximum in March 2018 (67.9%, 6.59, respectively). After a decrease in April 2018 and a gradual increase until July 2018, PUFA and UND decreased in August 2018 (59.3%, 4.56, respectively), and then increasing until October 2018 (Figure 4B and Supplementary Table S6).

TL extracted from the *C. cylindracea* from the mixed and monospecific settlement co-varied and was considerably higher in the thalli of the mixed settlement, except in August 2018. Generally, maximum values were reached in February (mixed:

$22.5 \pm 1.0 \text{ mg g}^{-1} \text{ DW}$ , monospecific:  $19.5 \pm 1.1 \text{ mg g}^{-1} \text{ DW}$ ) and minimum in August 2018 (mixed:  $7.2 \pm 1.5 \text{ mg g}^{-1} \text{ DW}$ , monospecific:  $10.2 \pm 1.3 \text{ mg g}^{-1} \text{ DW}$ , Figure 4A). The percent distributions of dominant components among the fatty acids were seasonally stable. Saturates represented the major fraction of total fatty acids in the mixed (30.1–93.7%) and monospecific (29.7–70.3%) settlements, except for February 2018, and were always dominated by C16:0 and to a lesser extent, by C14:0. MUFA was mostly represented by C16:1(n-7) and C18:1(n-9). PUFA varied inversely to SAT, reaching the maximum in February and minimum in August 2018 in mixed (3.0–55.5%) and monospecific (19.4–54.6%) settlements. PUFA were dominated by C18:3(n-3) with an important contribution of C18:2(n-6), C16:3(n-3), C20:5(n-3), and C20:4(n-6) fatty acids (Supplementary Table S7). UND increased until February 2018, when it started to decline until March to May 2018. In *C. cylindracea* of both sites, a considerably lower UND were

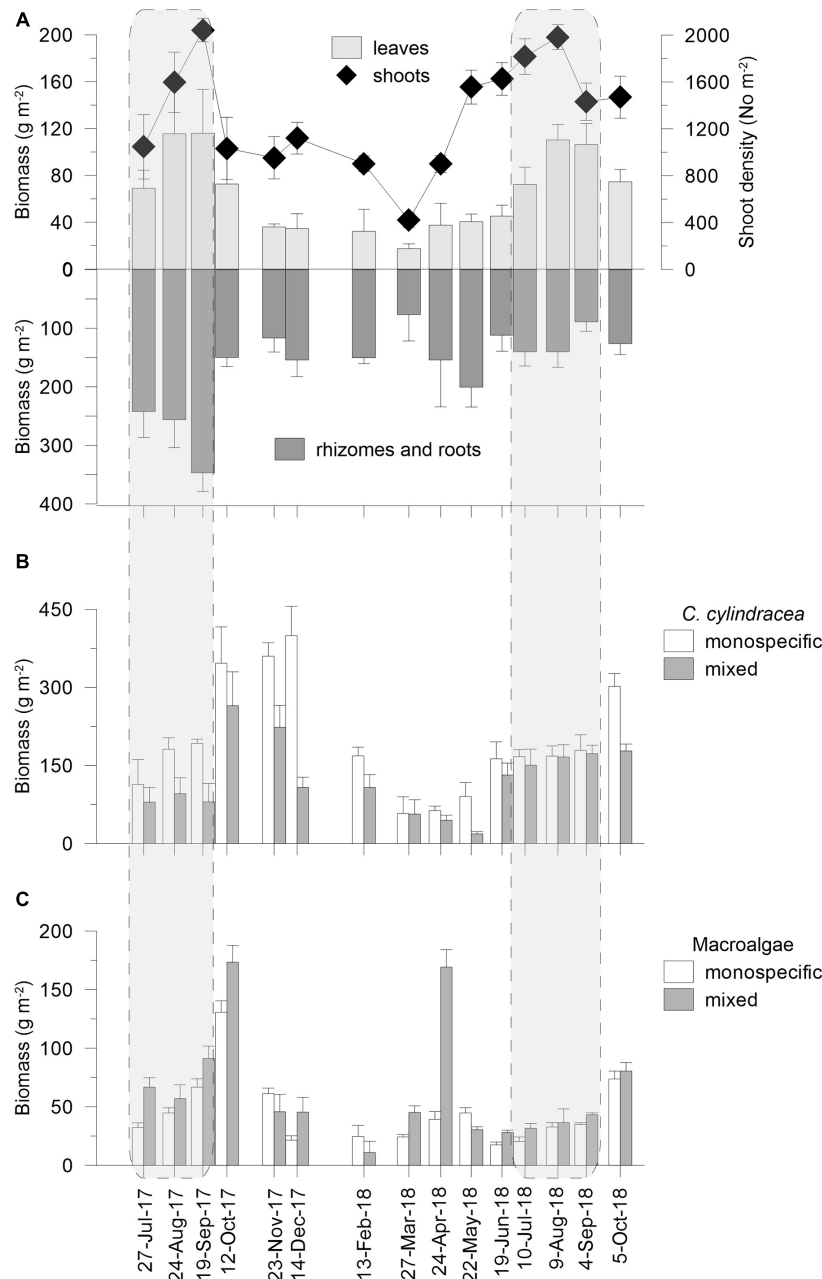


**FIGURE 3** | Above- and below-ground biomass and shoot density of *C. nodosa* in the meadow invaded by *C. cylindracea*—mixed settlement **(A)**, biomass of *C. cylindracea* in its monospecific and in the mixed settlement **(B)**; biomass of macroalgae in the *C. cylindracea* monospecific settlement and in the mixed settlement **(C)**, during investigated period. Data are presented as mean  $\pm$  SD ( $n = 3$ ).

observed in July and August 2018 than during the rest of the study period (**Figure 4B**).

## Sediment Granulometric Composition

According to the granulometric composition, the vegetated (underlying mixed and monospecific settlements) and non-vegetated sediments were classified as slightly gravelly muddy sand. Given the median grain sizes ( $d_g$ ) and

permeability ( $k$ ), the vegetated sediments were fine-grained ( $d_g < 165 \mu\text{m}$ ) with low permeability ( $k < 2.10^{-11} \text{m}^2$ ), while the non-vegetated sediment was classified as medium-grained ( $165 \mu\text{m} < d_g < 379 \mu\text{m}$ ) and permeable ( $2.10^{-11} \text{m}^2 < k < 10^{-10} \text{m}^2$ ). Generally, the  $d_g$  distribution showed a shift toward coarser particles from the sediment surface until 4 cm and from the sediments of the mixed to monospecific settlements and to the non-vegetated sediment (**Figure 5**).

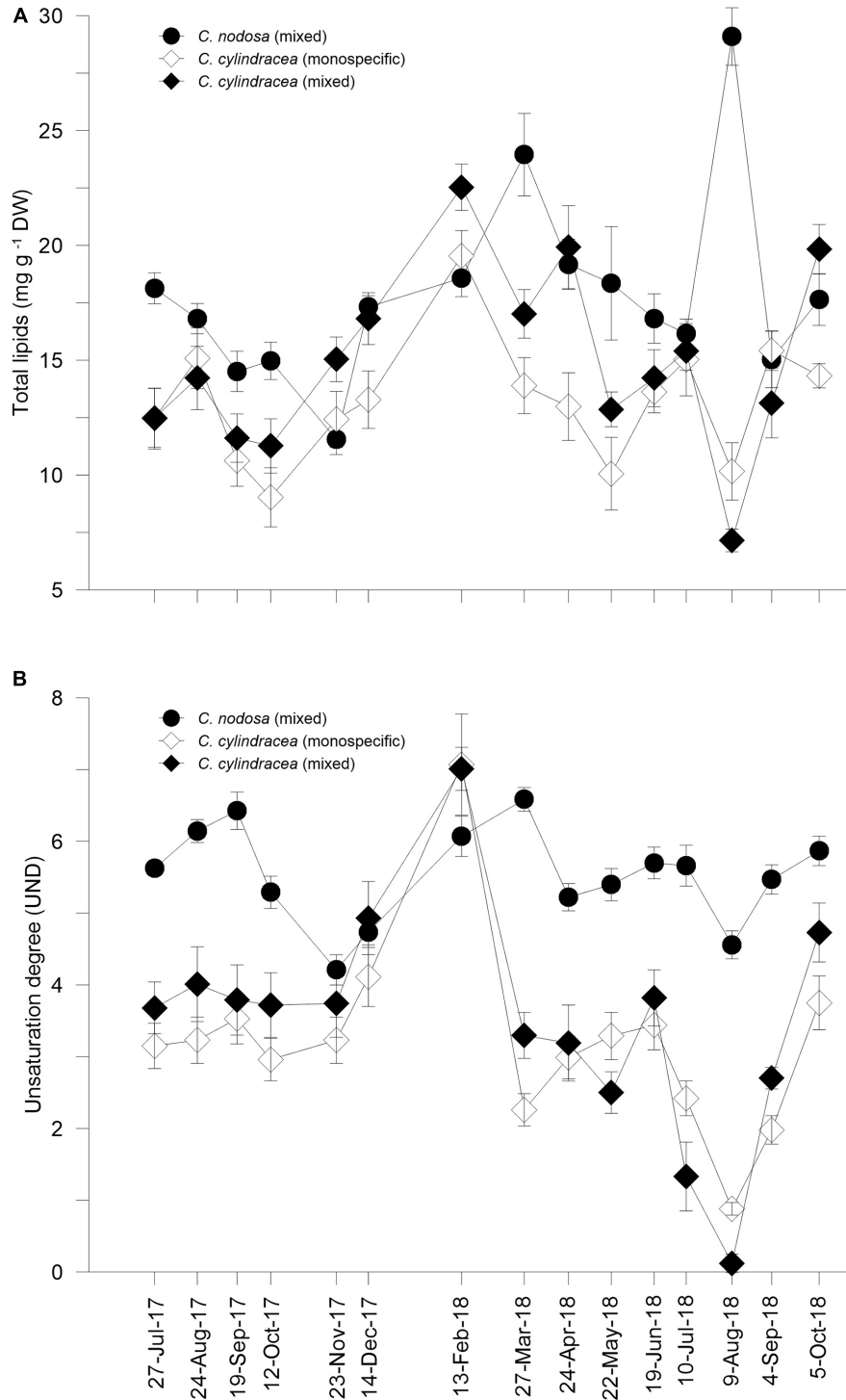


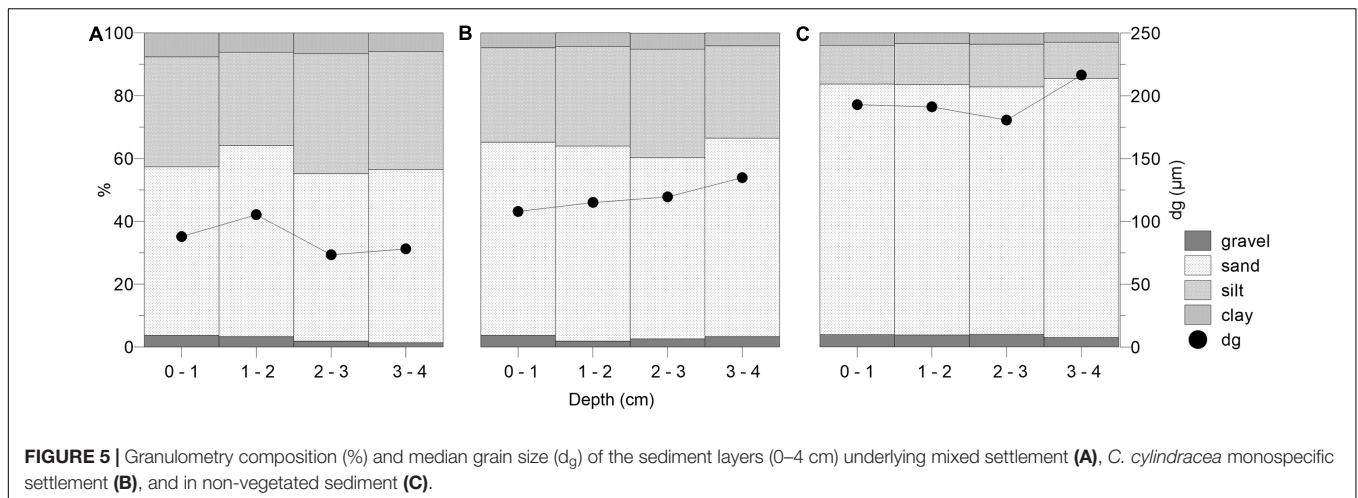
**FIGURE 4 |** Total lipid concentrations (A) and unsaturation degree (B) in *C. nodosa* leaves and *C. cylindracea* thalli in the mixed and monospecific settlement during investigated period. Data are presented as mean ± SD (TL, n = 3; UND, n = 2–3).

**Oxygen (O<sub>2</sub>), Redox Potential (E<sub>h</sub>), Hydrogen Sulfide (H<sub>2</sub>S), and Elemental Sulfur (S<sup>0</sup>)**

Oxygen concentrations (O<sub>2</sub>) in the bottom water of the monospecific settlement (0.1 ± 0.2 to 126.8 ± 30.0 μM)

were lower than in the mixed settlement (38.9 ± 25.1 to 195.8 ± 5.9 μM) or above non-vegetated sediment (111.5 ± 4.8 to 198.8 ± 5.1 μM). At all three sites, the variations of oxygen content relative to saturation level (O<sub>2</sub>/O<sub>2 sat</sub>) throughout the





sampling period were generally similar. In the monospecific settlement, the bottom waters were hypoxic in July and August 2017 and in April, May, and July 2018, while in the mixed settlement in September and October 2018 (Figure 6A). Similar monthly variations in  $O_2$  concentrations were observed in the sediment (0–4 cm) at all stations reaching their maximum  $O_2$  concentrations during March and April 2018. Lower values and narrower ranges of  $O_2$  were found in the sediment below the monospecific settlement ( $0$  to  $17.6 \pm 24.7 \mu\text{M}$ ) than below mixed settlements ( $0.5 \pm 0.5$  to  $68.6 \pm 97.1 \mu\text{M}$ ) and non-vegetated ( $1.5 \pm 1.3$  to  $49.9 \pm 39.6 \mu\text{M}$ ) sediments.

The redox transition depth (RTD,  $E_h \leq 0$ ) showed a similar trend in all sediments, being generally shallower below the *C. cylindracea* monospecific settlement (Figure 6B). In sediments below mixed (8–28 mm), monospecific settlements (4–19 mm), and non-vegetated sediment (14–30 mm), RTDs gradually deepened from July 2017 to March 2018. Afterward it progressed abruptly toward the sediments surface in April to May 2018 followed by moderate fluctuations until September 2018. During summer 2018, in the sediment below the mixed settlement, RTD (5–7 mm) was shallower than during the summer of 2017 (8–9 mm). In contrast, RTDs were similar in both seasons below the *C. cylindracea* monospecific settlement (2017: 4–7 mm; 2018: 0–7 mm) and in non-vegetated sediment (2017: 15–17 mm; 2018: 18–20 mm).  $E_h$  differed between stations, being more negative in the sediment below the monospecific settlement than in the other sediments.

Concentrations of free  $H_2S$  in sediment pore water generally increased with depth. Below the mixed settlement, the  $H_2S$  concentrations (up to  $29.49 \pm 10.18 \mu\text{M}$ ) showed a more pronounced and frequent formation of accumulation zones, between the surface and 2 cm of sediment depth. Such appearances were recorded in December 2017, and in May 2018 with  $H_2S$  rising to the surface of sediment and intruding into bottom waters in September 2018, when the highest concentrations were measured (up to  $90.8 \pm 30.5 \mu\text{M}$ ). For  $H_2S$  concentrations in the monospecific settlement (up to  $36.8 \pm 10.6 \mu\text{M}$ ), the elevation toward the sediment surface was recorded in April 2018 and then in July 2018 when

it appeared in bottom waters (Figure 7). In non-vegetated sediment,  $H_2S$  concentrations (up to  $7.4 \pm 3.1 \mu\text{M}$ ) were generally low (data not shown). During summer 2018, in the sediment below the mixed settlement  $H_2S$  concentrations were higher and accumulation fronts shallower than during summer 2017.

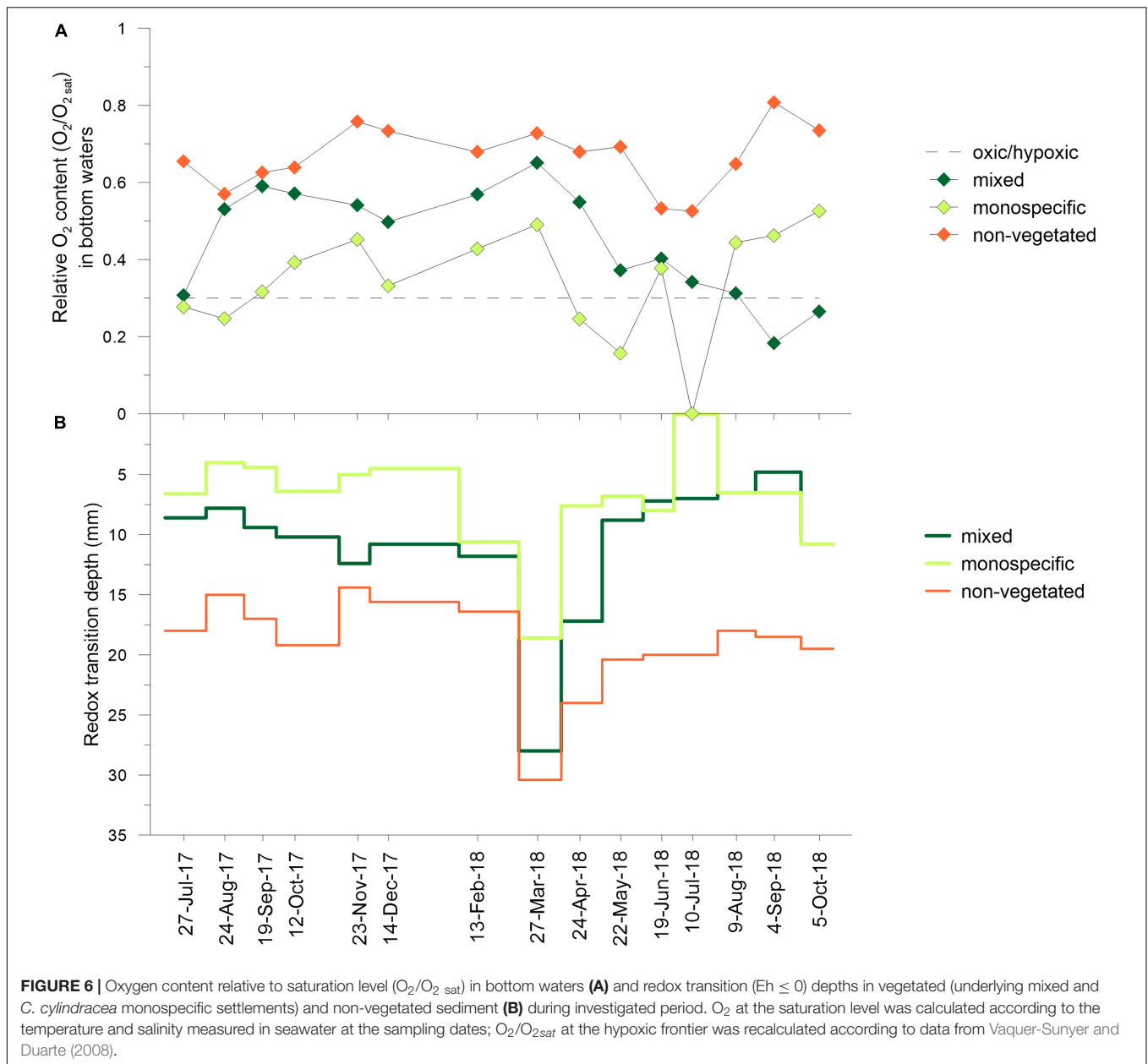
The ranges of approximated  $S^0$  concentrations in the sediment below the monospecific settlement ( $0.01$ – $0.23 \text{ mg}\cdot\text{g}^{-1} \text{ DW}$ ) were higher than below mixed settlement ( $0.01$ – $0.09 \text{ mg}\cdot\text{g}^{-1} \text{ DW}$ ) and in the non-vegetated sediment ( $0$ – $0.03 \text{ mg}\cdot\text{g}^{-1} \text{ DW}$ , data not shown). In all sediments, the concentrations of  $S^0$  generally varied in opposite mode to  $H_2S$  concentrations, being lower in  $H_2S$  accumulation zones.

### Prokaryotic Abundance

Prokaryotic abundance in the sediment layers (0–4 cm) underlying the mixed settlement ( $15.8 \pm 3.3$  to  $33.4 \pm 2.7 \cdot 10^7$  cells  $\text{g}^{-1}$  fresh weight, FW) was similar to the sediment below the monospecific settlement ( $16.8 \pm 1.1$  to  $29.9 \pm 4.5 \cdot 10^7$  cells  $\text{g}^{-1}$  FW). Both vegetated sediments displayed a significantly higher abundance than the non-vegetated ( $12.9 \pm 1.6$  to  $18.8 \pm 1.9 \cdot 10^7$  cells  $\text{g}^{-1}$  FW) sediment (Supplementary Table S8). In all sediments, PA was lower during the winter and spring (February to May 2018). After an increase in June 2018, high PA was maintained throughout the summer of 2018 in all sediments, being significantly higher than during the summer of 2017 (Supplementary Table S8 and Supplementary Figure S2A).

### Total Lipids (TL)

The concentrations of total lipids in the surface sediments below the mixed ( $1.15 \pm 0.08$  to  $1.62 \pm 0.10 \text{ mg}\cdot\text{g}^{-1} \text{ DW}$ ), monospecific ( $1.00 \pm 0.07$  to  $1.22 \pm 0.09 \text{ mg}\cdot\text{g}^{-1} \text{ DW}$ ) settlements and non-vegetated sediments ( $0.38 \pm 0.04$  to  $0.55 \pm 0.14 \text{ mg}\cdot\text{g}^{-1} \text{ DW}$ ) differed significantly, being ranked as mixed > monospecific > non-vegetated. During the summer of 2018, TL in the sediments at all sites were significantly lower in comparison to the summer of 2017 (Supplementary Table S8 and Supplementary Figure S2B).



### Relationship Between Environmental Parameters in Vegetated Sediments

The relationships between  $H_2S$ , Eh,  $O_2$ ,  $S^0$ , TL, and PA in sediments underlying mixed and monospecific settlements were analyzed using a PCA. PC1 explained 51.1% and PC2 23.1% of the variability (Figure 8). PC1 separated most of the sediments below the mixed settlement (except the sediments from June to September 2018) according to higher concentrations of  $O_2$ , TL, and more positive Eh from most of the sediments below the monospecific settlement (except the sediments in February and March 2018). The monospecific settlement was characterized by higher PA and  $S^0$  concentrations. On PC2, more negative Eh, higher  $H_2S$ , and lower  $S^0$  concentrations caused the separation of sediments below the mixed (May to September 2018) and

monospecific settlement (April and July 2018) from all other samples (Figure 8).

## DISCUSSION

### *C. nodosa* in Control of the Growth of *C. cylindracea*

The presence of *C. cylindracea* in the meadow did not affect the shoot density and the above-ground biomass of *C. nodosa* throughout the study period. Invaded meadow of *C. nodosa* showed consistent seasonal fluctuations reaching the highest above-ground biomass in the summers of 2017 and 2018, the lowest in winter, and exhibited exponential growth in spring as

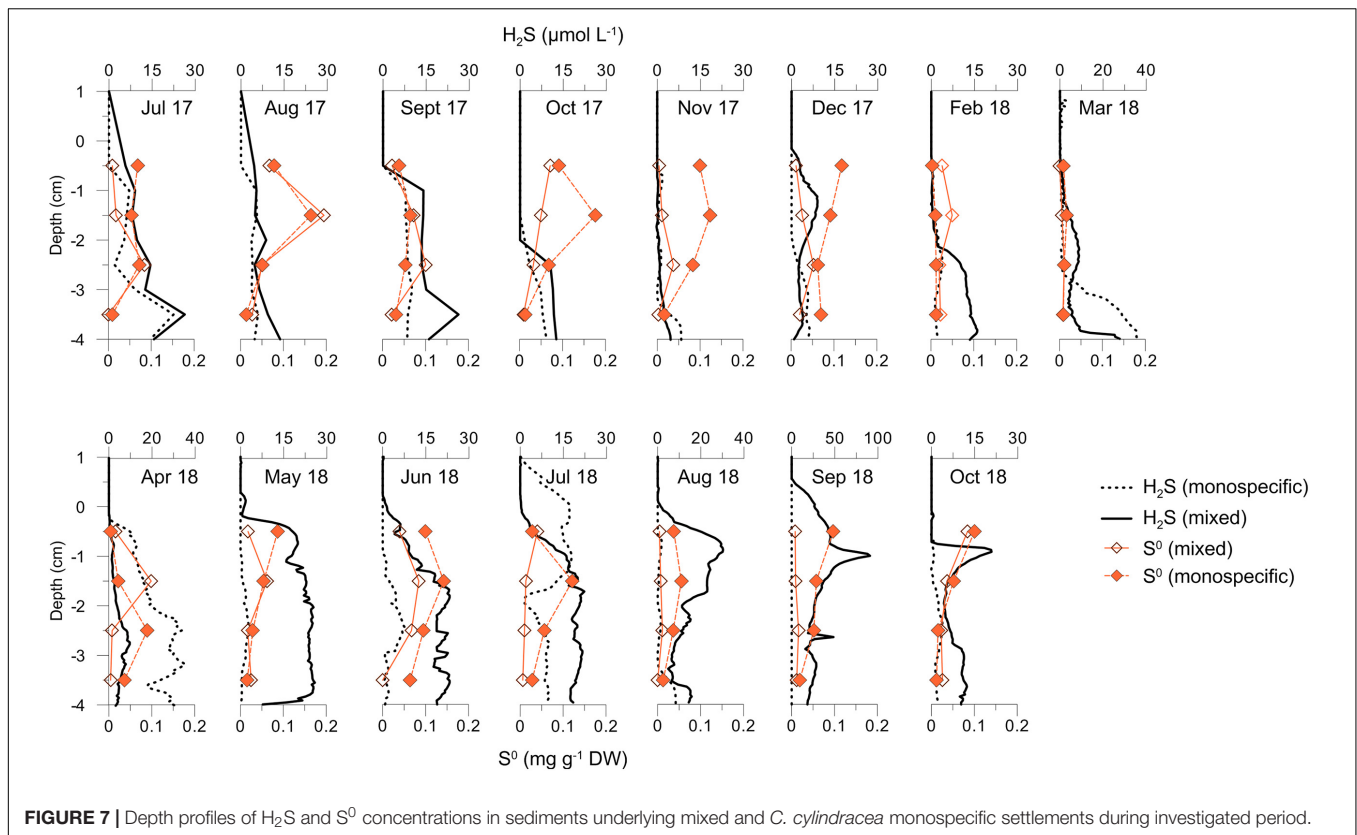


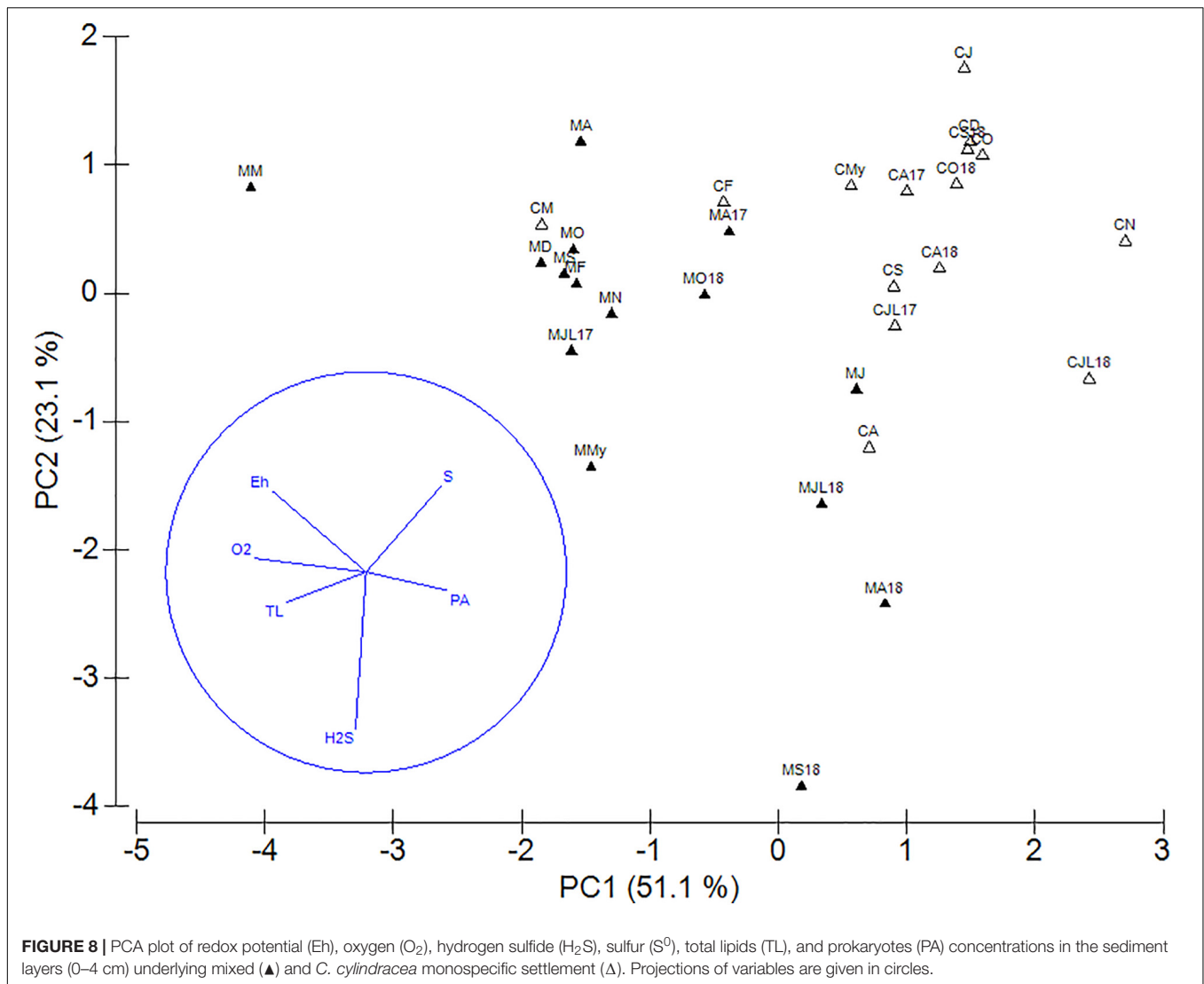
**FIGURE 7** | Depth profiles of  $H_2S$  and  $S^0$  concentrations in sediments underlying mixed and *C. cylindracea* monospecific settlements during investigated period.

commonly observed for this species in monospecific meadows (Terrados and Ros, 1992; Zavodnik et al., 1998; Agostini et al., 2003). Likewise, the seasonal cycle of *C. cylindracea* in both settlements, with increasing biomass from summer to autumn, a drastic regression in winter and a renewed growth in spring occurred as reported for other temperate areas (Piazzi and Cinelli, 1999; Ceccherelli et al., 2000; Iveša and Devescovi, 2006; Blažina et al., 2009). However, our results showed that during 2017 *C. cylindracea* biomass in the mixed settlement was lower than in its monospecific stands. This finding could be ascribed to the shading provided by *C. nodosa* leaves and to the reduced availability of open substrate for *C. cylindracea* rhizoid attachment in the *C. nodosa* meadow. The contribution of the macroalgae to the effects of shading and open substrate reduction on *C. cylindracea* growth was larger in the mixed settlement, most probably due to the significantly higher biomass in comparison to the monospecific settlement.

Shading by reduction of incident light attenuates or even prevents photosynthesis, retarding the growth and decreasing the biomass production of autotrophs (Pardal-Souza et al., 2017). As a physiological response to a shaded habitat, *C. cylindracea* in the mixed settlement generally accumulated more lipids and showed a higher unsaturation of the thalli in comparison to the monospecific one predominantly during the intensive meadow growth. By increased unsaturation, membrane fluidity is increased and the electron transport in the photosystem is facilitated to approach optimal photosynthetic activity under low light

conditions (Guschina and Harwood, 2009; Wacker et al., 2016; Beca-Carretero et al., 2019).

*Caulerpa cylindracea*, like other rhizophytic algae, tends to bury their rhizoids in the sediment for nutrient acquisition, thus gaining an advantage over non-rhizophytic macroalgae relying only on the nutrients from the water column. In contrast with other rooted primary producers, such as seagrasses, *C. cylindracea* competes for nutrients from the water and from the sediment. The ability of *Caulerpa* to take up and translocate nutrients from the sediment supports its biomass production (Williams, 1984) and spreading over the bare sediment (Alexandre and Santos, 2020) and assists the growth and development of the monospecific settlement. This nutrient uptake ability of *Caulerpa* is critical since low-nutrient conditions generally characterize the coastal waters of western Istria (Ivančić et al., 2018). In contrast, *C. cylindracea* in the mixed settlement, in addition to competition for nutrients, faced a reduced availability of free sediment for rhizoid burial due to the overwhelming presence of *C. nodosa* below-ground tissue. The reduced open substrate and therefore insufficient support with nutrients from the sediment most likely caused a decrease in biomass after substantial proliferation in October 2017, in contrast to the *C. cylindracea* settlement where high biomass was maintained until December 2017. Previous research showed that in healthy growing seagrass meadows, invasive macroalgae, regardless of their biomass, have little effect on sediment biogeochemistry or habitat modification (Holmer et al., 2009). Thus, while the resistance to the invasion of intact seagrass beds, such as those of *Posidonia oceanica*,



has primarily been attributed to light limitation (Glasby, 2013; Marín-Guirao et al., 2015), the success of the invasion might also be controlled by the limited availability of sediment substrate. Therefore, the lack of open substrate was crucial factor in limiting *C. cylindracea* growth within the meadow during 2017, since the shading provided by *C. nodosa* leaves and macroalgae continually affected this understory species during the entire study period.

The sediments underlying the mixed settlements showed a higher organic enrichment than those below the monospecific stands, suggesting that the combined effect of both macrophytes increased the sediment organic pools and enhanced the trapping of organic matter (Piazzini et al., 2007). Their different granulometric composition additionally emphasizes this divergence in organic matter enrichment between the two sediments. The absorptive capacity for organic molecules and the degree of organic matter preservation was higher in the mixed area due to the smaller grain size of the sediment. Generally higher H<sub>2</sub>S concentrations and shallower depths of the sulfide front were found below the invaded meadow in

comparison to the sediment below *C. cylindracea* monospecific stands (Figure 7). However, in the monospecific settlement, lower oxygen concentrations, more negative Eh coupled with RTD closer to the sediment surface were observed. The oxygen depletion in *C. cylindracea* sediment might be explained by a considerably higher S<sup>0</sup> concentration likely derived from more intense sulfide oxidation. This process could indicate a rapid and efficient removal of the produced sulfide by the chemical reaction with free oxygen or more likely mediated by sulfide-oxidizing bacteria (Jørgensen, 1977; Cúcio et al., 2016). Additionally, the presence of densely packed thalli covering the sediment surface limited the oxygen diffusion and penetration into the sediment. By the simultaneous consumption of H<sub>2</sub>S and O<sub>2</sub> highly reducing conditions near the sediment surface are created.

In contrast, in the sediment under the mixed settlement, the deeper RTD might be related to a below-ground tissue due to the vertical coupling between its biomass and positive redox anomaly (Enríquez et al., 2001). A more extensive sediment layer with oxic conditions (Eh > 0) accompanied with a more positive redox



potential was probably caused by the better oxygenation of the sediment due to radial oxygen leakage from the *C. nodosa* below-ground tissue along with O<sub>2</sub> diffusion from bottom waters in contact with the meadow (Holmer et al., 2006). The difference between the RTDs of the monospecific and mixed settlements was more pronounced until December 2017 (Figure 6) when both macrophytes were declining in biomass. During the winter/early spring, H<sub>2</sub>S production decreased in both settlements, likely due to the reduced activity of sulfate-reducing prokaryotes at lower temperatures, and the sediments gradually shifting toward a more oxidized state. H<sub>2</sub>S detected within the rooted area of the invaded meadow could be attributed to the presence of reducing micro-niches where anaerobic metabolism could occur irrespective of surrounding redox conditions (Jørgensen, 1977; Frederiksen and Glud, 2006). By rapid desaturation of increasing lipids, both macrophytes increased their cell membranes fluidity to achieve chilling resistance at lower temperatures (Guschina and Harwood, 2009). In both settlements, *C. cylindracea* survived winter temperatures in the form of small thallus fragments (rhizoids, stolons, and propagules). Similar and less drastic reductions in biomass were also reported in warmer regions of the Mediterranean Sea (Ceccherelli et al., 2000; Piazzini et al., 2001). Thus, the mild winter with short-lasting low temperatures (below 9°C) likely allowed a faster recovery and growth of *C. cylindracea* during the spring (Iveša et al., 2015).

The bloom of macroalgae within the invaded *C. nodosa* meadow in April 2018 (Figure 3C) most likely contributed to prolong the regression of *C. cylindracea* until May 2018, in contrast to the monospecific settlement where its growing phase started earlier (Figure 3B). Filamentous macroalgae, which in April 2018 contributed noticeably to the meadow cover (Supplementary Figure S1), generally grow better than other morpho-functional groups due to their higher nutrient uptake rates (Pedersen and Borum, 1997; Taylor et al., 1998). These macroalgae likely exploited this advantage in the competition for nutrients with *C. cylindracea*, that was still in dormant phase when the metabolic needs are at a minimum, and monopolized the available substrate. This short-term burst in macroalgal biomass followed by a steep decrease in biomass (Figure 3C) suggests that at least a part of this material became available for degradation.

### ***C. cylindracea* Proliferation Led to the Alteration of Sediment Conditions and Disturbance of the Stability of the *C. nodosa* Meadow**

In April and May 2018, *C. nodosa* entered its growth phase. The shoot density along with below-ground tissue considerably increased. The sediment nutrient uptake by small seagrass species, such as *C. nodosa*, is closely dependent on nutrients regenerated from recently deposited organic matter (Duarte et al., 1998). In May 2018, an increase in temperature and availability of the macroalgal remains probably stimulated the activity of sulfate-reducing prokaryotes and the release of nutrients along with H<sub>2</sub>S production leading to the development of more reducing conditions. From June onward, the conditions in the

invaded meadow sediment shifted to a new regime, characterized by expanding anoxia closer to the sediment surface, that became similar to that under the *C. cylindracea* monospecific settlement (Figures 6, 8). Such highly reducing sediment conditions had been likely stimulated by a production of new and very active rhizoid clusters buried in the sediments. Already in June 2018, *C. cylindracea* proliferated in both settlements and their biomasses became very similar. *C. nodosa* responded to the newly established sediment conditions by decreasing the below-ground tissue biomass while shoot density and above-ground biomass continued to increase. It seems very likely that anoxia driven by *C. cylindracea* proliferation severely reduced or even prevented the translocation of photoassimilates and the transport of photosynthetically produced oxygen from leaves and shoots to the rhizomes and roots (Zimmerman and Alberte, 1996; Alcoverro et al., 1999). In accordance, the energy production in the roots was impaired (Smith et al., 1988). Since *C. nodosa* cannot tolerate such long-lasting anoxia without reserves imported from the above-ground tissue, the reduction of below-ground biomass is likely unavoidable. Such unbalanced growth in which *C. nodosa* kept a more substantial fraction of CO<sub>2</sub> fixation in the photosynthetic compartment and was not stored as reserves lasted until October 2018 (Figure 3A). This resulted in considerably higher above- to below-ground biomass ratios than observed during the summer of 2017 and reported for healthy growing and stable *C. nodosa* meadows (Duarte et al., 1998; Cebrián et al., 2000). Therefore, the control of *C. cylindracea* over *C. nodosa* was supported by its alteration of the below-ground processes, as *Caulerpa* species are regularly abundant in disturbed seagrass beds and their decaying patches (Holmer et al., 2009; Glasby, 2013; Ceccherelli et al., 2014; Gribben et al., 2018).

During July and August 2018 *C. cylindracea* likely underwent spawning. The release of gametes, which has a high energetic cost, resulted in degraded thalli condition manifested by discoloration. Such conditions were evidenced by a considerably decreased UND of thalli (Figure 4B), which derived from the sharp depletion of PUFAs, most likely due to their incorporation into gametes enabling their long-term viability (Clifton, 1997). The spawning was likely triggered by large fluctuations in daily temperatures that *C. cylindracea* faced in July and August 2018 unlike during the same period in 2017 (Figure 2B) when only vegetative propagation occurred. However, the greater decrease in physiological indices of *C. cylindracea* in the meadow, matching to its poorer condition, suggests that a comparatively larger part of the population spawned than in the monospecific settlement. This difference could be ascribed to a wider range of day-night temperature oscillations (Figure 2C) combined with a milder hydrodynamic regime due to the flow reduction of the waters by the seagrass leaves, which is more favorable for spawning algae (Pearson and Serrao, 2006). During the spawning, no decrease in *C. cylindracea* biomass was observed in either settlement. However, it is possible that energy invested in this process, especially in the mixed settlement became unavailable for growth in early autumn in contrast to the previous year. Unexpectedly, macroalgae displayed a lack of biomass increase in both settlements. While the temperature and

its large oscillations might have also influenced their growth cycle, the impaired physiological condition of the *C. cylindracea* might have contributed as well, but the exact mechanism remains unclear. However, the resulting poor competitive ability of *C. cylindracea* due to exhaustion by spawning was likely exploited by filamentous macroalgae as their contribution in the cover of both settlements was strikingly higher than in the previous summer (**Supplementary Figure S1**). The temperature fluctuations did not have a major effect on the conditions of *C. nodosa* above-ground tissues. Only a moderate decrease in the degree of unsaturation was observed (**Figure 4B**), presenting a typical metabolic adjustment to a sudden increase in temperature (up to 29.34°C) in August 2018. A similar response of seagrass was observed during an experiment where *C. nodosa* and *P. oceanica* were exposed to a heat wave reaching a plateau of 29°C (Beca-Carretero et al., 2018) which is comparable to our field conditions. *C. nodosa* tolerates heat stress by sustaining enhanced photosynthesis, an ability allowing its growth and persistence in shallow environments (Marín-Guirao et al., 2016; Nguyen et al., 2020).

In September 2018, the minimized or even disrupted root respiration of the reduced below-ground tissue biomass likely enabled a H<sub>2</sub>S penetration into the plant, causing a strong shedding of the shoots. During October 2018, the conditions in the water column and sediment returned to a sustainable state favorable for the recovery of rhizomes. The slight increase in shoot density indicated that *C. nodosa* might have regained its fitness likely due to the increased below-ground biomass and the re-establishment of more balanced growth. This revitalization accompanied with the lack of invasive macroalgae growth might have increased the stability of the meadow, thereby re-exerting its control over *C. cylindracea* growth and propagation.

## Ecological Significance

Our results showed that the changes in the sediment conditions, caused by invasive *C. cylindracea* proliferation, appear to be the main factor that affected the decrease in *C. nodosa* below-ground biomass production, thus disrupting the stability of the seagrass meadow. The presence of *C. cylindracea* did not affect the *C. nodosa* above-ground biomass and shoot density. The invaded seagrass meadow appears to keep or even enhance its trapping of particles and thereby, increasing water clarity and providing protection against coastal erosion. However, the presence of *C. cylindracea* might change the biodiversity and secondary production of foraging benthic species since the invaded meadow does not provide the same trophic and nursery support as the monospecific *C. nodosa* habitats (Williams, 2007; Bulleri et al., 2010). Therefore, changes in the structural complexity of the coastal ecosystem where these two macrophytes coexist could be expected.

Even though *C. nodosa* is a protected species (UNEP-PAM-RAC/SPA, 2012) and an important biological element of coastal water quality included in European directives and monitoring programs (Orlando-Bonaca et al., 2015), its invaded meadows should receive more attention. The prolonged destabilization of the invaded meadows could increase their susceptibility to coastal modification and water quality degradation which are

considered the main causes of *C. nodosa* decline and extinction as reported in European coastal areas including the northern Adriatic (Tuya et al., 2014; de los Santos et al., 2019; Orlando-Bonaca et al., 2019; Najdek et al., 2020). So far, containment of *C. cylindracea* was not successful and further spread along the Adriatic coast can be expected. For these reasons, invaded meadows should be considered as more vulnerable habitats and given a higher monitoring priority. In particular, the results of our study present an early warning to our local/regional authorities to implement policies and strategies to prevent further coastal destruction (e.g., touristic facilities, mechanical damage by dredging and anchoring) and mitigate the impact of existing anthropogenic activities (e.g., untreated and uncontrolled release of wastewaters) negatively affecting the quality of coastal waters. Further studies of *C. nodosa* and *C. cylindracea* interactions at larger spatial and temporal scales are needed to predict and evaluate the stability, conservation, and sustainability of the functions and services provided by invaded *C. nodosa* meadows to the shallow coastal areas.

## DATA AVAILABILITY STATEMENT

The original contributions presented in the study are included in the article/**Supplementary Material**. Further inquiries can be directed to the corresponding author/s.

## AUTHOR CONTRIBUTIONS

MN, MK, and GH contributed to conceptualization. MK, PP, MM, II, LI, IF, and MN contributed to investigation. MN contributed to formal analysis and writing—original draft. MK, GH, PP, LI, II, IF, and MM contributed to writing—review and editing. All authors contributed to the article and approved the submitted version.

## FUNDING

The financial support was provided by the Croatian Science Foundation to MN (project IP-2016-06-7118, MICRO-SEAGRASS). GH was supported by grants of the Austrian Science Fund (ARTEMIS; #P28781-B21 and Microbial Nitrogen Cycling; # W1257-B20).

## ACKNOWLEDGMENTS

We sincerely thank J. Jakovčević and M. Buterer for nutrient and chlorophyll *a* determination, and A. Budiša and I. Haberle for occasional help during separation and biometry of plant material.

## SUPPLEMENTARY MATERIAL

The Supplementary Material for this article can be found online at: <https://www.frontiersin.org/articles/10.3389/fmars.2020.602055/full#supplementary-material>

## REFERENCES

- Agostini, S., Pergent, G., and Marchand, B. (2003). Growth and primary production of *Cymodocea nodosa* in a coastal lagoon. *Aquat. Bot.* 76, 185–193. doi: 10.1016/s0304-3770(03)00049-4
- Alcoverro, T., Zimmerman, R. C., Kohrs, D. G., and Alberte, R. S. (1999). Resource allocation and sucrose mobilization in light-limited eelgrass *Zostera marina*. *Mar. Ecol. Prog. Ser.* 187, 121–131. doi: 10.3354/meps187121
- Alexandre, A., and Santos, R. (2020). High nitrogen and phosphorous acquisition by belowground parts of *Caulerpa prolifera* (Chlorophyta) contribute to the species' rapid spread in Ria Formosa lagoon, Southern Portugal. *J. Phycol.* 56, 608–617. doi: 10.1111/jpy.12988
- Beca-Carretero, P., Guihéneuf, F., Marín-Guirao, L., Bernardeau-Esteller, J., García-Muñoz, R., Stengel, D. B., et al. (2018). Effects of an experimental heat wave on fatty acid composition in two Mediterranean seagrass species. *Mar. Pollut. Bull.* 134, 27–37. doi: 10.1016/j.marpolbul.2017.12.057
- Beca-Carretero, P., Guihéneuf, F., Winters, G., and Stengel, D. B. (2019). Depth-induced adjustment of fatty acid and pigment composition suggests high biochemical plasticity in the tropical seagrass *Halophila stipulacea*. *Mar. Ecol. Prog. Ser.* 608, 105–117. doi: 10.3354/meps12816
- Blažina, M., Iveša, L. J., and Najdek, M. (2009). *Caulerpa racemosa*: adaptive varieties studied by fatty acid composition (Northern Adriatic Sea, Vrsar, Croatia). *Eur. J. Phycol.* 44, 183–189. doi: 10.1080/09670260802428250
- Boudouresque, C. F., Bernard, G., Pergent, G., Shili, A., and Verlaque, M. (2009). Regression of Mediterranean seagrasses caused by natural processes and anthropogenic disturbances and stress: a critical review. *Bot. Mar.* 52, 395–418. doi: 10.1515/bot.2009.057
- Bulleri, F., Balata, D., Bertocci, I., Tamburello, L., and Benedetti-Cecchi, L. (2010). The seaweed *Caulerpa racemosa* on Mediterranean rocky reefs: from passenger to driver of ecological change. *Ecology* 91, 2205–2212. doi: 10.1890/09-1857.1
- Cebrián, J., Pedersen, M. F., Kroeger, K. D., and Valiela, I. (2000). Fate of production of the seagrass *Cymodocea nodosa* in different stages of meadow formation. *Mar. Ecol. Prog. Ser.* 204, 119–130. doi: 10.3354/meps204119
- Ceccherelli, G., and Cinelli, F. (1997). Short-term effects of nutrient enrichment of the sediment and interactions between the seagrass *Cymodocea nodosa* and the introduced green alga *Caulerpa taxifolia* in a Mediterranean bay. *J. Exp. Mar. Biol. Ecol.* 217, 165–177. doi: 10.1016/s0022-0981(97)00050-6
- Ceccherelli, G., and Cinelli, F. (1999). Effects of *Posidonia oceanica* canopy on *Caulerpa taxifolia* size in a north-western Mediterranean bay. *J. Exp. Mar. Biol. Ecol.* 240, 19–36. doi: 10.1016/s0022-0981(99)00044-1
- Ceccherelli, G., Piazzini, L., and Cinelli, F. (2000). Response of the non-indigenous *Caulerpa racemosa* (Forsskål) J. Agardh to the native seagrass *Posidonia oceanica* (L.) Delile: effect of density of shoots and orientation of edges of meadows. *J. Exp. Mar. Biol. Ecol.* 243, 227–240. doi: 10.1016/s0022-0981(99)00122-7
- Ceccherelli, G., Pinna, S., Cusceddu, V., and Bulleri, F. (2014). The role of disturbance in promoting the spread of the invasive seaweed *Caulerpa racemosa* in seagrass meadows. *Biol. Inv.* 16, 2737–2745. doi: 10.1007/s10530-014-0700-7
- Chisholm, J. R. M., and Moulin, P. (2003). Stimulation of nitrogen fixation in refractory organic sediments by *Caulerpa taxifolia* (Chlorophyta). *Limnol. Oceanogr.* 48, 787–794. doi: 10.4319/lo.2003.48.2.0787
- Clifton, K. E. (1997). Mass spawning by green algae on coral reefs. *Science* 275, 1116–1118. doi: 10.1126/science.275.5303.1116
- Cline, J. D. (1969). Spectrophotometric determination of hydrogen sulfide in natural waters. *Limnol. Oceanogr.* 14, 454–458. doi: 10.4319/lo.1969.14.3.0454
- Cormaci, M., Furnari, G., and Giaccone, G. (2004). “Macrophytebenthos,” in *Mediterranean Marine Benthos: A Manual of Methods for Its Sampling and Study*, eds M. C. Gambi and M. Dappiano (Genova: Società Italiana di Biologia Marina), 217–246.
- Cúcio, C., Engelen, A. H., Costa, R., and Muyzer, G. (2016). Rhizosphere microbiomes of European seagrasses are selected by the plant, but are not species specific. *Front. Microbiol.* 7:440. doi: 10.3389/fmicb.2016.00440
- de los Santos, C. B., Krause-Jensen, D., Alcoverro, T., Marbà, N., Duarte, C. M., van Katwijk, M. M., et al. (2019). Recent trend reversal for declining European seagrass meadows. *Nat. Commun.* 10:3356. doi: 10.1038/s41167-019-11340-4
- De Villelle, X., and Verlaque, M. (1995). Changes and degradation in *Posidonia oceanica* bed invaded by the introduced tropical alga *Caulerpa taxifolia* in the northwestern Mediterranean. *Bot. Mar.* 38, 79–87.
- Duarte, C. M., Kennedy, H., Marbà, N., Gacia, E., Fourqurean, J. W., Beggs, J., et al. (2013). Seagrass community metabolism: assessing the capacity of seagrass meadows for carbon burial: current limitations and future strategies. *Ocean Coast. Manag.* 83, 32–38. doi: 10.1016/j.ocecoaman.2011.09.001
- Duarte, C. M., Merino, M., Agawin, N. S. R., Uri, J., Fortes, M. D., Gallegos, M. E., et al. (1998). Root production and belowground seagrass biomass. *Mar. Ecol. Prog. Ser.* 171, 97–108. doi: 10.3354/meps171097
- Enríquez, S., Marbà, N., Duarte, C. M., van Tussenbroek, B. I., and Reyes-Zavala, G. (2001). Effects of seagrass *Thalassia testudinum* on sediment redox. *Mar. Ecol. Prog. Ser.* 219, 149–158. doi: 10.3354/meps219149
- Epstein, S. S., and Rossel, J. (1995). Enumeration of sandy sediment bacteria: search for optimal protocol. *Mar. Ecol. Prog. Ser.* 117, 289–298. doi: 10.3354/meps117289
- Folk, R. L. (1954). The distinction between grain size and mineral composition in sedimentary-rock nomenclature. *J. Geol.* 62, 344–359. doi: 10.1086/626171
- Frederiksen, M. S., and Glud, R. N. (2006). Oxygen dynamics in the rhizosphere of *Zostera marina*: a two-dimensional planar optode study. *Limnol. Oceanogr.* 51, 1072–1083. doi: 10.4319/lo.2006.51.2.1072
- Gallucci, F., Hutchings, P., Gribben, P., and Fonseca, G. (2012). Habitat alteration and community-level effects of an invasive ecosystem engineer: a case study along the coast of NSW, Australia. *Mar. Ecol. Prog. Ser.* 449, 95–108. doi: 10.3354/meps09547
- Gambi, M. C., Nowell, A. R. M., and Jumars, P. A. (1990). Flume observations on flow dynamics in *Zostera marina* (eelgrass) beds. *Mar. Ecol. Prog. Ser.* 61, 159–169. doi: 10.3354/meps061159
- Gangi, A. F. (1985). Permeability of unconsolidated sands and porous rocks. *J. Geophys. Res. Solid* 90, 3099–3104. doi: 10.1029/jb090ib04p03099
- Garcias-Bonet, N., Marbà, N., Holmer, M., and Duarte, C. M. (2008). Effects of sediment sulfides on seagrass *Posidonia oceanica* meristematic activity. *Mar. Ecol. Prog. Ser.* 372, 1–6. doi: 10.3354/meps07714
- Glasby, T. M. (2013). *Caulerpa taxifolia* in seagrass meadows: killer or opportunistic weed? *Biol. Inv.* 15, 1017–1035. doi: 10.1007/s10530-012-0347-1
- Gribben, P. E., Thomas, T., Pusceddu, A., Bonechi, L., Bianchelli, S., Buschi, E., et al. (2018). Below-ground processes control the success of an invasive seaweed. *J. Ecol.* 106, 2082–2095. doi: 10.1111/1365-2745.12966
- Guschina, I. A., and Harwood, J. (2009). “Algal lipids and effect of environment on their biochemistry,” in *Lipids in Aquatic Ecosystems*, eds M. Arts, M. Brett, and M. Kainz (New York, NY: Springer), 1–24. doi: 10.1007/978-0-387-89366-2\_1
- Holmer, M., Marbà, N., Lamote, M., and Duarte, C. M. (2009). Deterioration of sediment quality in seagrass meadows (*Posidonia oceanica*) Invaded by Macroalgae (*Caulerpa* sp.). *Estuar. Coast.* 32, 456–466. doi: 10.1007/s12237-009-9133-4
- Holmer, M., Pedersen, O., and Ikejima, K. (2006). Sulfur cycling and sulfide intrusion in mixed Southeast Asian tropical seagrass meadows. *Bot. Mar.* 49, 91–102. doi: 10.1515/bot.2006.013
- Holm-Hansen, O., Lorenzen, C. J., Holmes, R. W., and Strickland, J. D. H. (1965). Fluorometric determination of chlorophyll. *J. Conseil.* 301, 3–15. doi: 10.1093/icesjms/30.1.3
- Ivančić, I., Paliaga, P., Pfannkuchen, M., Đakovac, T., Najdek, M., Steiner, P., et al. (2018). Seasonal variations in extracellular enzymatic activity in marine snow-associated microbial communities and their impact on the surrounding water. *FEMS Microbiol. Ecol.* 94:fyi198. doi: 10.1093/femsec/fiy198
- Iveša, L., Blažina, M., and Najdek, M. (2004). Seasonal variation in fatty acid composition of *Caulerpa taxifolia* (M. Vahl.) C. Ag. in the northern Adriatic Sea (Malinska, Croatia). *Bot. Mar.* 47, 209–214. doi: 10.1515/BOT.2004.021
- Iveša, L., and Devescovi, M. (2006). Seasonal vegetation patterns of the introduced *Caulerpa racemosa* (Caulerpaceae, Chlorophyta) in the northern Adriatic Sea (Vrsar, Croatia). *Period. Biol.* 108, 111–116. doi: 10.1127/nova.hedwigia/50/1990/111
- Iveša, L., Djakovac, T., and Devescovi, M. (2015). Spreading patterns of the invasive *Caulerpa cylindracea* Sonder along the west Istrian Coast (northern Adriatic Sea, Croatia). *Mar. Environ. Res.* 107, 1–7. doi: 10.1016/j.marenvres.2015.03.008



- Jørgensen, B. B. (1977). The sulfur cycle of a coastal marine sediment (Limfjorden, Denmark). *Limnol. Oceanogr.* 22, 814–832. doi: 10.4319/lo.1977.22.5.0814
- Khotimchenko, S. V. (1995). Fatty acid composition of green algae of the genus *Caulerpa*. *Bot. Mar.* 38, 509–512. doi: 10.1515/botm.1995.38.1-6.509
- Littler, M. M., and Littler, D. S. (1984). Relationships between macroalgal functional form groups and substrata stability in a subtropical rocky-intertidal system. *J. Exp. Mar. Biol. Ecol.* 74, 13–34. doi: 10.1016/0022-0981(84)90035-2
- Marín-Guirao, L., Bernardeau-Esteller, J., Ruiz, J. M., and Sandoval-Gil, J. M. (2015). Resistance of *Posidonia oceanica* seagrass meadows to the spread of the introduced green alga *Caulerpa cylindracea*: assessment of the role of light. *Biol. Inv.* 17, 1989–2009. doi: 10.1007/s10530-015-0852-0
- Marín-Guirao, L., Ruiz, J. M., Dattolo, E., Garcia-Munoz, R., and Procaccini, G. (2016). Physiological and molecular evidence of differential short-term heat tolerance in Mediterranean seagrasses. *Sci. Rep.* 6:28615. doi: 10.1038/srep28615
- McKinnon, J. G., Gribben, P. E., Davis, A. R., Jolley, D. F., and Wright, J. T. (2009). Differences in soft-sediment macrobenthic assemblages invaded by *Caulerpa taxifolia* compared to uninhabited habitats. *Mar. Ecol. Prog. Ser.* 380, 59–71. doi: 10.3354/meps07926
- MICROMERITICS (2002). *SediGraph 5100 Particle Size Analysis System Operator Manual*. Norcross: Micromeritics Instrument Corporation.
- Najdek, M., Korlević, M., Paliaga, P., Markovski, M., Ivančić, I., Iveša, L., et al. (2020). Dynamics of environmental conditions during a decline of a *Cymodocea nodosa* meadow. *Biogeosciences* 17, 3299–3315. doi: 10.5194/bg-17-3299-2020
- Nguyen, H. M., Kim, M., Ralph, P. J., Marín-Guirao, L., Pernice, M., and Procaccini, G. (2020). Stress memory in seagrasses: first insight into the effects of thermal priming and the role of epigenetic modifications. *Front. Plant Sci.* 11:494. doi: 10.3389/fpls.2020.00494
- Orlando-Bonaca, M., Francé, J., Mavrič, B., Grego, M., Lipej, L., Flander Putrle, V., et al. (2015). A new index (MediSkew) for the assessment of the *Cymodocea nodosa* (Ucria) Ascherson meadow's status. *Mar. Environ. Res.* 110, 132–141. doi: 10.1016/j.marenvres.2015.08.009
- Orlando-Bonaca, M., Francé, J., Mavrič, B., and Lipej, L. (2019). Impact of the port of Koper on *Cymodocea nodosa* meadow. *Annales* 29, 187–194.
- Orth, R. J., Carruthers, T. J. B., Dennison, W. C., Duarte, C. M., Fourqurean, J. W., Heck, K. L. Jr., et al. (2006). A global crisis for seagrass ecosystems. *BioScience* 56, 987–793.
- Panayotidis, P., and Žuljević, A. (2001). Sexual reproduction of the invasive green alga *Caulerpa racemosa* var. *occidentalis* in the Mediterranean Sea. *Oceanol. Acta* 24, 199–203. doi: 10.1016/s0399-1784(01)01142-2
- Pardal-Souza, A. L., Dias, G. M., Jenkins, S. R., Ciotti, Á.M., and Christofoletti, R. A. (2017). Shading impacts by coastal infrastructure on biological communities from subtropical rocky shores. *J. Appl. Ecol.* 54, 826–835. doi: 10.1111/1365-2664.12811
- Pearson, G. A., and Serrao, E. A. (2006). Revisiting synchronous gamete release by fucoid algae in the intertidal zone: fertilization success and beyond? *Int. Comp. Biol.* 46, 587–597. doi: 10.1093/icb/ic1030
- Pedersen, M. F., and Borum, J. (1997). Nutrient control of estuarine macroalgae: growth strategy and the balance between nitrogen requirements and uptake. *Mar. Ecol. Prog. Ser.* 161, 155–163. doi: 10.3354/meps161155
- Piazzi, L., and Balata, D. (2009). Invasion of alien macroalgae in different Mediterranean habitats. *Biol. Inv.* 11, 193–204. doi: 10.1007/s10530-008-9224-3
- Piazzi, L., Balata, D., Foresi, L., Cristaudo, C., and Cinelli, F. (2007). Sediment as a constituent of Mediterranean benthic communities dominated by *Caulerpa racemosa* var. *cylindracea*. *Sci. Mar.* 71, 129–135. doi: 10.3989/scimar.2007.71n1129
- Piazzi, L., Ceccherelli, G., and Cinelli, F. (2001). Threat to macroalgal diversity: effects of the introduced green alga *Caulerpa racemosa* in the Mediterranean. *Mar. Ecol. Prog. Ser.* 210, 149–159. doi: 10.3354/meps210149
- Piazzi, L., and Cinelli, F. (1999). Development and seasonal dynamics of a population of the tropical alga *Caulerpa racemosa* (Forsskål) J. Agardh in the Mediterranean. *Cryptogamie Algol.* 20, 295–300. doi: 10.1016/j.aquabot.2005.02.008
- Porter, K. G., and Feig, Y. S. (1980). The use of DAPI for identification and counting aquatic microflora. *Limnol. Oceanogr.* 25, 943–984. doi: 10.4319/lo.1980.25.5.0943
- Rasheed, M. A., and Unsworth, R. K. F. (2011). Long-term climate-associated dynamics of a tropical seagrass meadow: implications for the future. *Mar. Ecol. Prog. Ser.* 422, 93–103. doi: 10.3354/meps08925
- Rizzo, L., Pusceddu, A., Stabili, L., Alifano, P., and Fraschetti, S. (2017). Potential effects of invasive seaweed (*Caulerpa cylindracea*, Sonder) on sedimentary organic matter and microbial metabolic activities. *Sci. Rep.* 7:12113. doi: 10.1038/s41598-017-12556-4
- Samper-Villarreal, J., Lovelock, C. E., Saunders, M. I., Roelfsema, C., and Mumby, P. J. (2016). Organic carbon in seagrass sediment is influenced by seagrass canopy complexity, turbidity, wave height, and water depth. *Limnol. Oceanogr.* 61, 938–952. doi: 10.1002/lno.10262
- Smith, R. D., Pregnall, A. M., and Alberte, R. S. (1988). Effects of anaerobiosis on root metabolism of *Zostera marina* (eelgrass): implications for survival in reducing sediments. *Mar. Biol.* 98, 131–141. doi: 10.1007/bf00392668
- Strickland, J. D. H., and Parsons, T. R. (1972). A practical handbook of seawater analysis. *Bull. Fish. Res. Board. Can.* 167, 1–310.
- Tamburello, L., Maggi, E., Benedetti-Cecchi, L., Bellistri, G., Rattray, A. J., Ravaglioli, C., et al. (2015). Variation in the impact of non-native seaweeds along gradients of habitat degradation: a meta-analysis and an experimental test. *Oikos* 124, 1121–1131. doi: 10.1111/oik.02197
- Taylor, R. B., Peek, J. T. A., and Rees, T. A. V. (1998). Scaling of ammonium uptake by seaweeds to surface area:volume ratio: geographical variation and the role of uptake by passive diffusion. *Mar. Ecol. Prog. Ser.* 169, 143–148. doi: 10.3354/meps169143
- Terrados, J., and Ros, J. D. (1992). Growth and primary production of *Cymodocea nodosa* (Ucria) Ascherson in a mediterranean coastal lagoon: the Mar Menor (SE Spain). *Aquat. Bot.* 43, 63–74. doi: 10.1016/0304-3770(92)90014-A
- Tuya, F., Ribeiro-Leite, L., Arto-Cuesta, N., Coca, J., Haroun, R., and Espino, F. (2014). Decadal changes in the structure of *Cymodocea nodosa* seagrass meadows: natural vs. human influences. *Estuar. Coast. Shelf Sci.* 137, 41–49. doi: 10.1016/j.ecss.2013.11.026
- UNEP-PAM-RAC/SPA (2012). *Protocol Concerning Specially Protected Areas and Biological Diversity in the Mediterranean. Annex II. List of Endangered or Threatened Species*. Paris: UNEP.
- Vaquier-Sunyer, R., and Duarte, C. M. (2008). Thresholds of hypoxia for marine biodiversity. *PNAS* 105, 15452–15457. doi: 10.1073/pnas.0803833105
- Wacker, A., Piepho, M., Harwood, J. L., Guschina, I. A., and Arts, M. T. (2016). Light-induced changes in fatty acid profiles of specific lipid classes in several freshwater phytoplankton species. *Front. Plant Sci.* 7:264. doi: 10.3389/fpls.2016.00264
- Williams, S. L. (1984). Uptake of sediment ammonium and translocation in a marine green macroalga *Caulerpa cupressoides*. *Limnol. Oceanogr.* 29, 374–379. doi: 10.4319/lo.1984.29.2.0374
- Williams, S. L. (2007). Introduced species in seagrass ecosystems: status and concerns. *J. Exp. Mar. Biol. Ecol.* 350, 89–110. doi: 10.1016/j.jembe.2007.05.032
- Zavodnik, N., Travizi, A., and De Rosa, S. (1998). Seasonal variations in the rate of photosynthetic activity and chemical composition of the seagrass *Cymodocea nodosa* (Ucr.) Asch. *Sci. Mar.* 62, 301–309. doi: 10.3989/scimar.1998.62n4301
- Zimmerman, R. C., and Alberte, R. S. (1996). Effect of light/dark transition on carbon translocation in eelgrass *Zostera marina* seedlings. *Mar. Ecol. Prog. Ser.* 136, 305–309. doi: 10.3354/meps136305
- Žuljević, A., Antolić, B., and Onofri, V. (2003). First record of *Caulerpa racemosa* (*Caulerpales*: Chlorophyta) in the Adriatic Sea. *J. Mar. Biol. Assoc. UK* 83, 711–712. doi: 10.1017/s0025315403007689h

**Conflict of Interest:** The authors declare that the research was conducted in the absence of any commercial or financial relationships that could be construed as a potential conflict of interest.

Copyright © 2020 Najdek, Korlević, Paliaga, Markovski, Ivančić, Iveša, Felja and Herndl. This is an open-access article distributed under the terms of the Creative Commons Attribution License (CC BY). The use, distribution or reproduction in other forums is permitted, provided the original author(s) and the copyright owner(s) are credited and that the original publication in this journal is cited, in accordance with accepted academic practice. No use, distribution or reproduction is permitted which does not comply with these terms.